Influence of molecular-weight polydispersity on the glass transition of polymers

Shu-Jia Li, Shi-Jie Xie, Yan-Chun Li,* Hu-Jun Qian, and Zhong-Yuan Lu†
Institute of Theoretical Chemistry, State Key Laboratory of Supramolecular Structure and Materials, Jilin University, Changchun 130021, China

(Received 31 October 2015; revised manuscript received 25 December 2015; published 27 January 2016)

It is well known that the polymer glass transition temperature T_g is dependent on molecular weight, but the role of molecular-weight polydispersity on T_g is unclear. Using molecular-dynamics simulations, we clarify that for polymers with the same number-average molecular weight, the molecular-weight distribution profile (either in Schulz-Zimm form or in bimodal form) has very little influence on the glass transition temperature T_g, the average segment dynamics (monomer motion, bond orientation relaxation, and torsion transition), and the relaxation-time spectrum, which are related to the local nature of the glass transition. By analyzing monomer motions in different chains, we find that the motion distribution of monomers is altered by molecular-weight polydispersity. Molecular-weight polydispersity dramatically enhances the dynamic heterogeneity of monomer diffusive motions after breaking out of the "cage," but it has a weak influence on the dynamic heterogeneity of the short time scales and the transient spatial correlation between temporarily localized monomers. The stringlike cooperative motion is also not influenced by molecular-weight polydispersity, supporting the idea that stringlike collective motion is not strongly correlated with chain connectivity.

DOI: 10.1103/PhysRevE.93.012613

I. INTRODUCTION

Polymers are good glass formers due to their inherent difficulties in forming crystals, and they are often used as model systems to study the glass transition [1–4]. When approaching the glass transition temperature T_g, the microscopic structure of supercooled liquids varies only slightly, and glass is known as frozen liquids due to its similar microstructure with liquids [5–8]. However, its dynamic behavior changes dramatically: Relaxation time varies by more than ten orders of magnitude over a narrow temperature range near T_g [5–8]. It is still a challenge to provide a unified microscopic picture of the glass transition despite many years of extensive studies [5,6]. Research of the polymer glass transition is very important for both understanding the nature of the glass transition and the application of most industrial polymer products.

Most synthetic polymers have molecular-weight polydispersity, which has a dramatic influence on many features of polymers, such as phase behavior [9], rheology [10], and processing instabilities [11]. Molecular-weight polydispersity is also a vital factor influencing polymer mechanical properties, and T_g can be used as a single parameter to estimate the mechanical properties when defined consistently [12]. Whether there is any relation between T_g and molecular-weight polydispersity is very important for polymer applications and for understanding the nature of the glass transition. However, little attention has been paid to the influence of molecular-weight polydispersity on polymer T_g [2,13]. It is well known that T_g increases with molecular weight and saturates at high molecular weight, as illustrated in Fig. 1. This can be described by the Fox-Flory equation as $T_g = T_{g\infty} - K/M$. However, the origin of this dependence still remains elusive [14,15]. In practice, "the mass" in the above equation has been controversially taken as the number-average or the mass-average molecular weight. Previous research about the mass dependence of polymer T_g actually has not distinguished between them.

As an analogy with critical phenomena, there is an expectation that slower relaxation can be related to a growing length scale [16,17]. The growing cooperatively rearranging regions (CRRs) upon cooling are the cornerstone of the famous Adam and Gibbs (AG) [18] and random first-order transition (RFOT) [19] theories. However, the commonly used dynamic or static length scale [17,20–22] is relatively small, suggesting that it is a relatively local feature of the glass transition. The local segment dynamics and CRR analysis are necessary for understanding the influence of molecular-weight polydispersity on the polymer glass transition.

In addition, dynamic heterogeneity (DH) [23,24], which describes the spatial-temporal fluctuations in local dynamical behavior [16], is another key feature that characterizes glass formers. All disordered systems with glassy dynamics are reported with the existence of dynamic heterogeneity [16]. DH could be characterized by analyzing non-Gaussian parameters [25], multipoint correlations, and susceptibilities [6,16,26,27]. The analysis of the clusters of mobile and slow particles also provides a physical picture of DH [17]. Molecular-weight polydispersity inherently introduces the heterogeneity in the chain length. Whether this inherent heterogeneity influences the dynamic heterogeneity of supercooled polymer liquids is still an intriguing question.

Motivated by the above questions, we have systematically studied the glass transition of polymers with Schulz-Zimm as well as bimodal molecular-weight distributions using a bead-spring model [28,29] with molecular-dynamics simulations. The influence of molecular-weight distribution on the glass transition temperature, segment dynamics, CRRs, and DH have been clarified in detail. The paper is organized as follows: The details of the model and simulation method are presented in Sec. II. Then we present the results and analyze their implications in Sec. III. Finally, the paper ends with a discussion and conclusions in Sec. IV.

*liyanchun@jlu.edu.cn
†luzhy@jlu.edu.cn

II. MODEL CONSTRUCTION AND SIMULATION DETAILS

A. Model construction

In this study we have adopted the bead-spring model [28], which is a generic coarse-grained polymer model that is widely used in studies of the glass transition of polymers. This model has successfully reproduced many experimental phenomena [2,29–34]. Compared with all-atom models, we can access a larger length scale and time scale through this model, which provides an efficient way to study the general characteristics of polymeric glass formers [1]. In this model, monomers (represented by a "bead") that are not directly bonded interact with a truncated and shifted Lennard-Jones (LJ) potential,

$$U_{\mathrm{LJ}}(r) = 4\epsilon\left[\left(\frac{\sigma}{r}\right)^{12} - \left(\frac{\sigma}{r}\right)^{6}\right] + C(r_{\mathrm{cut}}). \quad (1)$$

Here, U_{LJ} is set to zero for $r > r_c = 2 \times 2^{1/6}\sigma$, and the constant C ensures that the potential vanishes continuously at r_c. Lennard-Jones units are employed, and all qualities are in reduced units, with length in units of σ, temperature in units of ϵ/k_B (k_B is the Boltzmann constant), and time in units of $(m\sigma^2/\epsilon)^{0.5}$. All the monomers are identical. Chain connectivity is controlled by a harmonic potential,

$$U_{\mathrm{bond}(r)} = \tfrac{1}{2}k_1(r - r_0)^2. \quad (2)$$

Here, $k_1 = 1111.0$ and $l_0 = 0.967$ [29]. The bending potential is defined as

$$U_{\mathrm{B}}(\theta) = \tfrac{1}{2}k_\theta(\theta - \theta_0)^2, \quad (3)$$

and the function form of the torsion potential is

$$U_{\mathrm{T}}(\phi) = \tfrac{1}{2}k_\phi[1 - \cos(3\phi)]. \quad (4)$$

Here, $\theta_0 = 120^\circ$, θ is the bending angle, and ϕ is the dihedral angle. Through tuning k_θ and k_ϕ, we can regulate chain rigidity, which can be characterized by persistent length:

$$l_p = \frac{l_0(C_\infty + 1)}{2}, \qquad C_\infty = \frac{1 - \cos(\theta)}{1 + \cos(\theta)}\frac{1 + \cos(\phi)}{1 - \cos(\phi)}. \quad (5)$$

Here, C_∞ is the characteristic ratio and l_0 is the average bond length [35]. Four kinds of chain rigidity are considered: $(k_\theta,k_\phi) = (0,0)$, (0.8754,0), (12,1), and (25,2), thus l_p takes values 1.27, 1.69, 1.78, and 1.94, respectively. It should be noted that l_p values of many real polymers can be found in the literature (normally in units of nm); however, l_p values in our generic model are in reduced units. The two kinds of l_p could not be compared directly. At the lowest temperature in our simulations, the maximum value of the bond-orientation order q_6 [36] is only about 0.14, hence our systems are safe from crystallization.

Following Ref. [29], we obtain the T_g's for polymer melts with different chain lengths for monodisperse polymers by using MD simulations. The dependence of T_g on the chain length of monodisperse polymers with different persistence lengths in our model is shown in Fig. 1. Apparently, T_g increases with increasing chain length, especially for chains with larger rigidity. To reflect the influence of the polydispersity index (PDI) on T_g, we focus on two number-average chain lengths ($\langle N\rangle$): $\langle N\rangle_1 = 12$ and $\langle N\rangle_2 = 40$, which are in the "increasing region" and "plateau region" in Fig. 1,

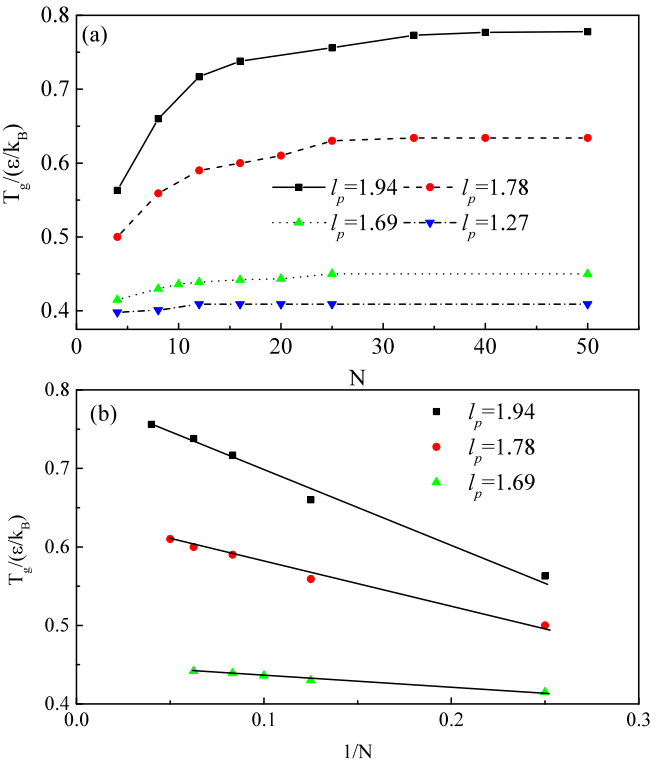

FIG. 1. (a) The chain length dependence of T_g for monodisperse polymers with different persistence lengths. (b) The fitting of $T_g \sim 1/N$ to the Fox-Flory equation. For $l_p = 1.69$, 1.78, and 1.94, the corresponding $T_{g\infty}$ are 0.45, 0.63, and 0.79, respectively. It is clear that the mass dependence of our bead spring chain model conforms to the Fox-Flory equation, which is in accordance with previous reports [14,15].

respectively. We consider two distribution forms: Schulz-Zimm (SZ) distribution and bimodal distribution, to represent chain length dispersity in this study. SZ distribution spreads from the uniform distribution (PDI = 1.0) to the most probable distribution (PDI = 2.0), defined as

$$f_w(x)dx = \frac{a^b x^{b-1} e^{-ax}}{\Gamma(b)}dx,\ M_n = \frac{b}{a},\ M_w = \frac{1+b}{a},$$
$$\mathrm{PDI} = \frac{M_w}{M_n} = 1 + \frac{1}{b}. \quad (6)$$

Here, x is a parameter describing the chain length, a and b are two adjustable parameters, and $\Gamma(b)$ is the Γ function of b. Figure 2 describes the variation of the Schulz-Zimm distribution with the PDI value for systems with $\langle N\rangle = 12$. According to Eq. (6), we generate a different number of polymer chains with required chain lengths to construct a polymer melt system with SZ molecular weight distribution. As for bimodal molecular weight distribution, we mix the short chains with the long chains according to the required PDI values; the details are shown in Table I.

B. Simulation details

In our simulations, there are around 18 000 monomers in each polymer system. We perform a stepwise isothermal-isobaric (NPT) cooling process with a step of $\Delta T = 0.03$

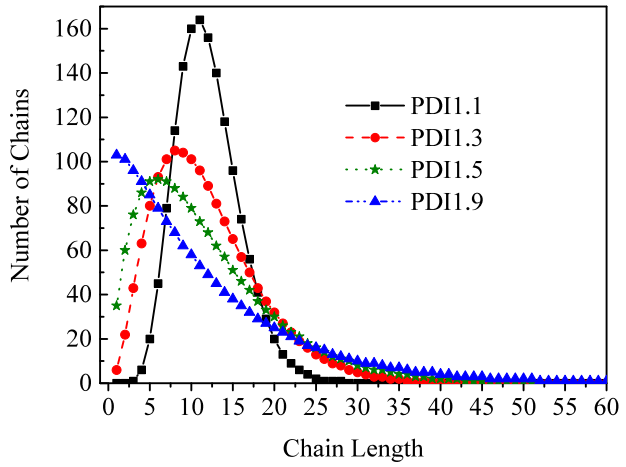

FIG. 2. The variation of Schulz-Zimm distribution for systems with $\langle N\rangle = 12$. It shows that with increasing PDI, both the number of short chains and the length of the longest chain increase. The total number of polymer chains is 1500.

from 1.1 to 0.2 for systems with $\langle N\rangle = 12$ and from 1.2 to 0.3 for systems with $\langle N\rangle = 40$; the pressure is set to 1.0. The equilibrium initial configurations are prepared at a higher temperature, $T = 2.0$. The Nosé-Hoover thermostat and Anderson barostat are used to control temperature and pressure, respectively. The time step for integrating the equations of motion is 0.001. The cooling rate can be roughly determined as 6×10^{-6}. We then perform isochoric-isothermal (NVT) simulations using the configurations obtained from NPT cooling runs with equilibrium densities as starting points. At each temperature, to guarantee that our systems are in equilibrium before data analysis, we have run simulations at least two times longer than the longest relaxation time when the monomer mean-square displacement (MSD) is comparable to the largest end-end mean-square distance R^2_{ee} of the longest chain in our systems. All the simulations are performed with periodic boundary conditions by using GALAMOST software [37].

III. RESULTS AND DISCUSSION

A. The glass transition temperature

Despite its dependence on preparation history, the glass transition temperature T_g is a vital property for polymers [8,12]. We locate T_g by measuring specific volume variation with T, and we adopt the function $\ln[v(T)] = c + dT$ (c,d are fitting parameters) to fit the data; see Refs. [29,38] for more details. The T_g value determined by the volumetric method is sensitive to the cooling rate. Compared with conventional experiments, our cooling rate is about a factor 10^8 faster. But extensive studies for a polymer model similar to the one used in this study shows that the cooling rate effects for these models are really weak [29]. Moreover, we adopt the same cooling process for systems with the same $\langle N\rangle$ to avoid the influence of the cooling rate on our conclusion. As Table II shows, once the number-average molecular weight and chain rigidity are fixed, the T_g value varies little between polymer systems with different chain length distribution forms and PDI values. The choice of chain rigidity l_p and number-average chain length $\langle N\rangle$ does not influence our conclusion. Although it had been reported in experiments that the PDI has very little influence on T_g for polydisperse polycarbonates [39], our result based on a generic polymer model clarifies that polymer T_g should be irrelevant to the PDI, even though T_g is dependent on the polymer molecular weight. As our model is independent of chemical details, our findings should apply to various polymers with linear chains. Moreover, as T_g is irrelevant to the PDI, the number average mass dependence of polydisperse polymers should be the same as that of monodisperse polymers (shown in Fig. 1).

TABLE I. The details of bimodal distribution. N and n represent the length and the number of chains, respectively. The subscripts 1 and 2 for N and n stand for the short chain and the long chain, respectively. The superscripts a and b of the PDI values indicate that systems are with $\langle N\rangle = 12$ and 40, respectively.

PDI:	1.444[a]	2.333[a]	5.0[a]	1.375[b]	2.43[b]	4.06[b]
N_1:	4	4	4	10	5	5
n_1:	750	1125	1350	180	292	360
N_2:	20	36	84	60	105	180
n_2:	750	375	150	270	148	90

TABLE II. The glass transition temperatures of polymers with different values of the PDI. The distribution forms without a superscript are Schulz-Zimm distributions. The distribution forms with superscript a are bimodal.

			$\langle N\rangle = 12$; ($l_p = 1.27$)			
PDI:	1.0	1.1	1.3	1.5		
T_g:	0.406	0.405	0.405	0.406		
			$\langle N\rangle = 12$; ($l_p = 1.69$)			
PDI:	1.0	1.1	1.3	1.5		
T_g:	0.439	0.440	0.440	0.438		
			$\langle N\rangle = 12$; ($l_p = 1.78$)			
PDI:	1.0	1.3	1.9	1.444[a]	2.333[a]	5.0[a]
T_g:	0.589	0.589	0.588	0.590	0.585	0.587
			$\langle N\rangle = 40$; ($l_p = 1.78$)			
PDI:	1.0	1.3	1.9	1.375[a]	2.43[a]	4.06[a]
T_g:	0.633	0.632	0.632	0.636	0.634	0.632
			$\langle N\rangle = 40$; ($l_p = 1.94$)			
PDI:	1.0	1.3	1.9	1.375[a]	2.43[a]	4.06[a]
T_g:	0.777	0.774	0.774	0.774	0.774	0.777

B. Dynamics

In the following, to study further the influence of chain length polydispersity on the glass transition, we take polymers with $l_p = 1.78$ and $\langle N\rangle = 12$ as an example. As Sec. III A shows, the choice of l_p and the average chain length do not influence the weak polydispersity dependence of T_g. The data for $l_p = 1.78$ are chosen to be shown here merely because these data are more representative as compared to the data for l_p either smaller or larger. In addition, as shown in Fig. 1, $N = 12$ is close to the "turning point" in the curve showing the

dependence of T_g on chain length. Chain length polydispersity may have more of an influence on the glass transition in this range. Therefore, we have chosen chains with $\langle N\rangle = 12$ as our main target system. We have also checked other choices of l_p and $\langle N\rangle$ and found that these choices do not influence our analyses. For simplicity, we show mainly the analyses for polymers with $l_p = 1.78$ and $\langle N\rangle = 12$ in the following.

In general, dynamics studies on the glass transition are conducted above the critical temperature of mode-coupling theory $T_{\rm MCT}$ [2,30–32,34]. Typically, $T_{\rm MCT} \approx 1.2 \times T_g$ [40]. For our systems with $l_p = 1.78$ and $\langle N\rangle = 12$, $1.2 \times T_g = 1.2 \times 0.59 = 0.71$. $T = 0.74$ is close to this value and is able to capture the dynamics related to the glass transition. Therefore, we choose it for most of the analyses in the following. Figure 3 shows the bond orientational autocorrelation function (ACF), defined as

$$P_2 = \tfrac{3}{2}\langle \vec{b}_j(0)\vec{b}_j(t)\rangle - 1, \tag{7}$$

and $P_{3\rm state}(t)$, defined as the probability of an average dihedral, has not visited all three states ($gauche^+$, $trans$, and $gauche^-$) after a time period t [41]. In this equation, $\vec{b}_j(t)$ is the jth bond vector at time t. Apparently, the molecular-weight polydispersity of polymers does not influence $P_2(t)$ and $P_{3\rm state}(t)$. Figure 4 shows the average MSD over all monomers, defined as

$$g_0(t) = \langle |r_i(t) - r_i(0)|^2\rangle, \tag{8}$$

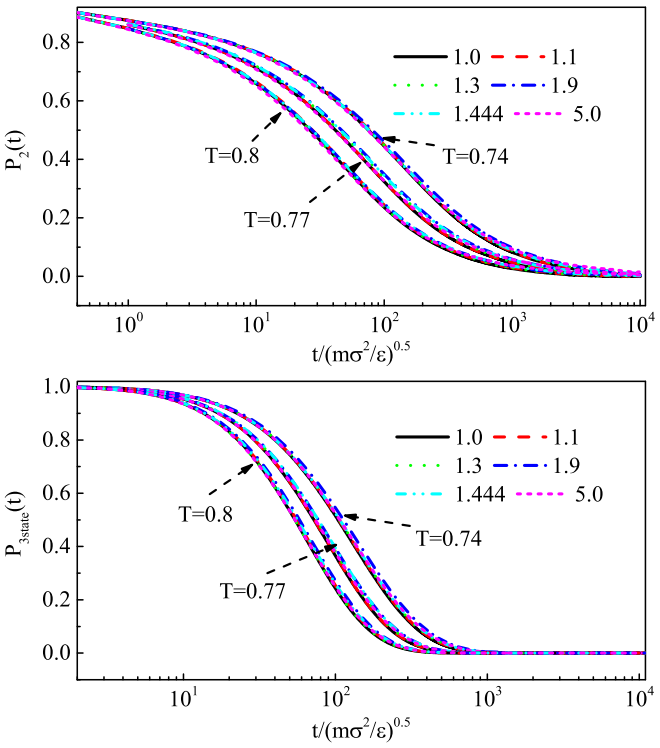

FIG. 3. (a) The bond orientational autocorrelation function, $P_2(t)$. (b) The probability that a dihedral has not visited all three states $gauche^+$, $trans$, and $gauche^-$ after a given time t, $P_{3\rm state}(t)$. The PDI values for SZ distribution are 1.1, 1.3, and 1.9. The PDI values for bimodal distribution are 1.444 and 5.0.

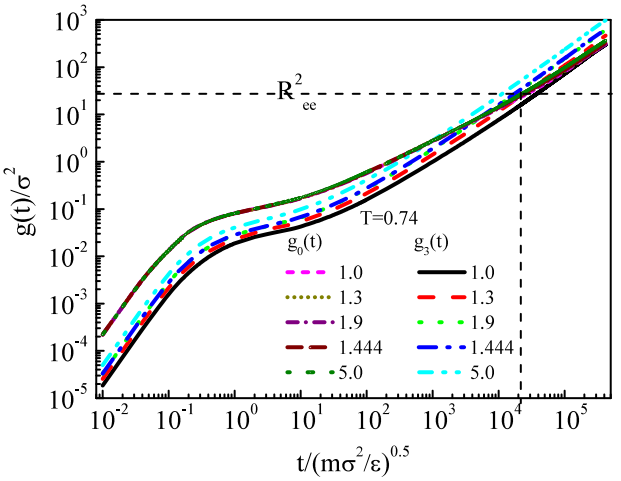

FIG. 4. The MSD over all monomers $g_0(t)$ and the MSD of the mass center of chains $g_3(t)$ for systems with various PDIs at $T = 0.74$. The PDI values for SZ distribution are 1.3 and 1.9. The PDI values for bimodal distribution are 1.444 and 5.0. We have also determined the number-average end-end mean-square distance $R^2_{\rm ee}$ for systems with various PDIs, and we find that the value, which is about $27\sigma^2$, is weakly influenced by polydispersity and temperature. Here, we use a dashed line to label the time when $g_0(t)$ is comparable to $R^2_{\rm ee}$, which is about $2.2 \times 10^4 (m\sigma^2/\epsilon)^{0.5}$.

where $r_i(t)$ is the position of the ith monomer, and the MSD of the mass center of chains $g_3(t)$,

$$g_3(t) = \left\langle \left| r_k^{\rm cm}(t) - r_k^{\rm cm}(0)\right|^2\right\rangle, \tag{9}$$

where $r_k^{\rm cm}(t)$ is the position of the mass center for the kth chain at time t. It is shown that the PDI does not influence monomer dynamics, but increasing the PDI results in faster chain dynamics in the condition with the same chain length distribution form. The influence of polydispersity on $g_3(t)$ is also related to the distribution form: $g_3(t)$ for the PDI1.444 system with bimodal distribution and $g_3(t)$ for the PDI1.9 system with SZ distribution almost converge. As we know, $g_0(t)$ describes monomer motion with time; $P_2(t)$ describes orientation variations of the bond, which is related to two connected monomers; $P_{3\rm state}(t)$ describes state variations of dihedral angle, which is related to four sequentially connected monomers. On the other hand, $g_3(t)$ represents the average chain motion for systems with various PDIs. Compared with $g_3(t)$, very little influence of chain length polydispersity on $g_0(t)$, $P_2(t)$, and $P_{3\rm state}(t)$ can be attributed to the fact that local relaxation properties are not sensitive to the difference in chain length distribution. Angell *et al.* have pointed out that, for polymers, the variation of volume is determined by liquid rearrangement to which "only fairly short range coordinated motions like the local segmental motions and the sub-Rouse modes" contribute [42]. Therefore, the irrelevance of local dynamics to chain length polydispersity means that polymer T_g is not affected by molecular-weight polydispersity.

As we can expect from their constructions, $g_0(t)$ will converge to $g_3(t)$ at long time scales for monodisperse systems, as Fig. 4 shows. However, a new phenomenon emerges for polydisperse systems: $g_3(t)$ surpasses $g_0(t)$ at long time scales. We can define the mobility of a monomer with chain length

L as D_{0L} and the mobility of a chain with length L as D_{3L}. Let $D_{0L} = g_0(t)$ and $D_{3L} = g_3(t)$ for monodisperse systems. For polydisperse systems, we define the fraction of chains with length L as ρ_{cL} and the fraction of monomers in the chains with length L as ρ_{mL}. Then $g_0(t) = \sum_k D_{0L_k}\rho_{mL_k}$ and $g_3(t) = \sum_k D_{3L_k}\rho_{cL_k}$. It is obvious that ρ_{cL_k} is larger than ρ_{mL_k} when L_k is smaller than the average chain length. As D_{0L_k} converges to D_{3L_k} at long time scales, to compare $g_0(t)$ and $g_3(t)$ we should focus on the distribution of the chain length. The fraction of shorter chains for constructing $g_3(t)$, which increases with the PDI in polydisperse systems with the same distribution form, is larger than the monomer fraction in the corresponding shorter chains for constructing $g_0(t)$. Therefore, $g_3(t)$ will exceed $g_0(t)$ in polydisperse systems at long time scales. The time that $g_3(t)$ exceeds $g_0(t)$ decreases with the PDI under the same distribution form. Our data for the PDI dependence of the monomer and the center-of-mass displacement are therefore consistent.

One definition of the α relaxation time τ_α is the time at which $g_0(\tau_\alpha) = 1$ [30,43–46]. It is the time that a monomer succeeds in leaving its nearest-neighbor "cage" and covers the distance of its own size [45,46]. Using this definition, we locate the mode-coupling transition temperature T_c at $T = 0.62$ from $\tau_\alpha \propto (T - T_c)^{-\gamma}$ [47], and we determine T_g as 0.54 from Vogel-Fulcher-Tammann (VFT) formula $\tau_\alpha = \tau_0 \exp[DT_0/(T - T_0)]$[$\tau_0 = 1$ and $\tau_\alpha(T_g) = 10^{14}$] [30]. The T_g value defined in this way is smaller than 0.59 determined through the specific volume method, as we can expect. The fitting temperatures for MCT and VFT fitting include 0.68, 0.69, 0.70, 0.71, 0.74, and 0.77. The effective cooling rate of VFT fitting is slower, and therefore a lower T_g value can be obtained, which is more in line with the experimental results. Once again, T_c and T_g determined in this way are independent of chain length polydispersity. The dynamic fragility D in the VFT formula describes how rapidly $\tau(T)$ changes with temperature; a larger value of D corresponds to less fragile glass formers [48]. We find that D, which is determined as 2.58 from the above VFT fitting, is apparently not altered by chain length polydispersity in this study. The α relaxation time can also be defined in other ways, such as through the intermediate scattering function $f_q(t)$:

$$f_q(t) = \left\langle \frac{1}{M} \sum_{j=1}^{M} e^{iq[r_j(t) - r_j(0)]} \right\rangle, \tag{10}$$

and the bond orientation autocorrelation function $P_2(t)$. We have defined the relaxation time through $f_q(\tau_\alpha) = 0.1$ [2]. The T_g (around 0.60) determined by VFT fitting using the same fitting temperatures as above and the relaxation time obtained from f_q are also not influenced by chain length polydispersity. Therefore, the definition of relaxation time will only alter the absolute value of T_g due to the well-known decoupling from the Stokes-Einstein relation, but not the qualitative conclusion [49,50].

The above relaxation times are average characteristic relaxation times. We can obtain the relaxation-time spectrum by analyzing $P_2(t)$ using the CONTIN method [51–54], where

$$P_2(t) = \int_{-\infty}^{+\infty} F[\ln(\tau)] \exp[-t/(\tau)] d(\ln \tau). \tag{11}$$

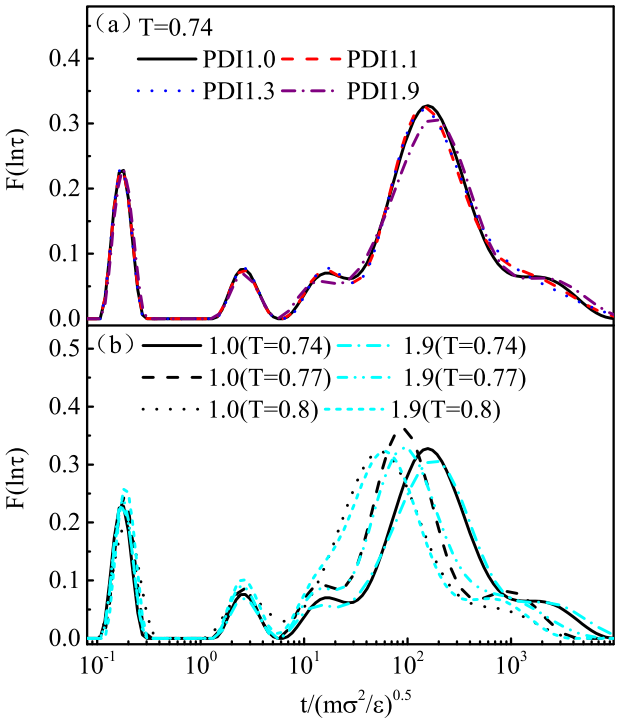

FIG. 5. The polydispersity (a) and temperature dependence (b) of the normalized distribution function of the relaxation times $F[\ln(\tau)]$ for $P_2(t)$.

Here, $F[\ln(\tau)]$ is a normalized distribution function of relaxation times. CONTIN is a general-purpose program for inverting noisy linear algebraic and integral equations by means of the inverse Laplace transform. It provides a simple method to obtain the inverse of Eq. (11) and get $F[\ln(\tau)]$. The peaks in the distribution function $F[\ln(\tau)]$ can be related to different processes in the relaxation-time spectrum. As Fig. 5 shows, at the temperatures in our study, we have observed three main relaxation peaks. The left and middle peaks correspond to secondary relaxations, which are weakly influenced by temperature. As Fig. 5(b) shows, the right peak is in the range of α relaxation [in the same range in which $P_2(t)$ relaxes to $1/e$], which shifts toward large time scales upon cooling. Figure 5(a) shows that all the peaks are basically independent of the PDI, which is consistent with our above observations.

C. Cooperative motion

According to AG and RFOT theories, a slower dynamics upon cooling accompanies a larger length scale (a larger scale of cooperative rearrangements), but both theories do not include a microscopic presentation of the nature of cooperative rearrangements. In recent years, several definitions of static and dynamic length scales that may be responsible for the growth of relaxation time scales were proposed [6,17]. Donati *et al.* found that mobile monomers are spatially correlated, and the mobile particles move cooperatively along stringlike paths at two different times [20], which give a physical picture for the growing length scale. According to Starr *et al.* [55], the string size [20,21,30,56] appears to be the most consistent measurement of CRRs for both AG and RFOT theories. Here,

we check the influence of chain length polydispersity on cooperative motion in our systems by analyzing the string size.

Following the procedures proposed in previous works [20,21,30,56], we have identified 6.5% of particles with the largest displacement over any chosen time range t as mobile particles [21,30,56]. For any two mobile monomers, if a monomer replaces the other within a radius δ over a period t, the two monomers are considered as being in the same string:

$$\min[|r_i(t) - r_j(0)|, |r_j(t) - r_i(0)|] < \delta. \tag{12}$$

Following Refs. [21,30], we choose $\delta = 0.55$; see Ref. [21] for more details. There are two different definitions of string size. One is the number-averaged string length $\langle S_n \rangle$:

$$\langle S_n \rangle = \frac{\sum_{s=1}^{\infty} s P(s)}{\sum_{s=1}^{\infty} P(s)}. \tag{13}$$

The other is the weight-averaged string length $\langle S_w \rangle$:

$$\langle S_w \rangle = \frac{\sum_{s=1}^{\infty} s^2 P(s)}{\sum_{s=1}^{\infty} s P(s)}. \tag{14}$$

Here, s is the string size and $P(s)$ is the probability of finding a string with length s. The ratio $\langle S_w \rangle / \langle S_n \rangle$, labeled as PDI_S, which is referred to as the PDI of strings, can describe the distribution of strings. Here, we use subscripts 1 and 2 to represent the cases with or without considering the string with $s = 1$, respectively. For example, $\langle S_{n2} \rangle$ is the number average string size without considering $s = 1$.

As Fig. 6(a) shows, the qualitative behaviors are quite similar for $\langle S_n \rangle$, $\langle S_w \rangle$, and the distribution of the string size PDI_S between the two cases. At short time scales, $\langle S_{n2} \rangle$ and $\langle S_{w2} \rangle$ are close to 2, and $\langle S_{n1} \rangle$ and $\langle S_{w1} \rangle$ are close to 1, respectively, which means that at short time scales the mobile monomers are not correlated. In the range between β and α relaxation, the string size and the dispersity of the string size distribution PDI_S are the largest. After breaking out of the cage, the mobile monomers are diffusive and do not tend to replace each other, so the average string size is decreasing.

Figure 7 shows the temperature dependence of the string size and its distribution for the monodisperse and polydisperse system, respectively. The position of the peak moves to larger time scales with decreasing temperature, implying a slower relaxation. The peak value grows upon cooling, supporting the idea that a slower relaxation is accompanied by a growing length scale. This behavior is similar for both monodisperse and polydisperse systems. We also find that chain length polydispersity does not influence the evolution of the string size and the distribution of the string size, as shown in Fig. 6(b). Previous research [21] showed that stringlike collective motion is not strongly correlated with chain connectivity. As chain length polydispersity is related to chain connectivity, our results are consistent with this observation. As we can find, the string size in our systems is relatively small (the largest of $\langle S_{w2} \rangle < 3$), i.e., the CRR length scale is rather small compared to the average chain length, suggesting the local nature of the glass transition of polymer systems.

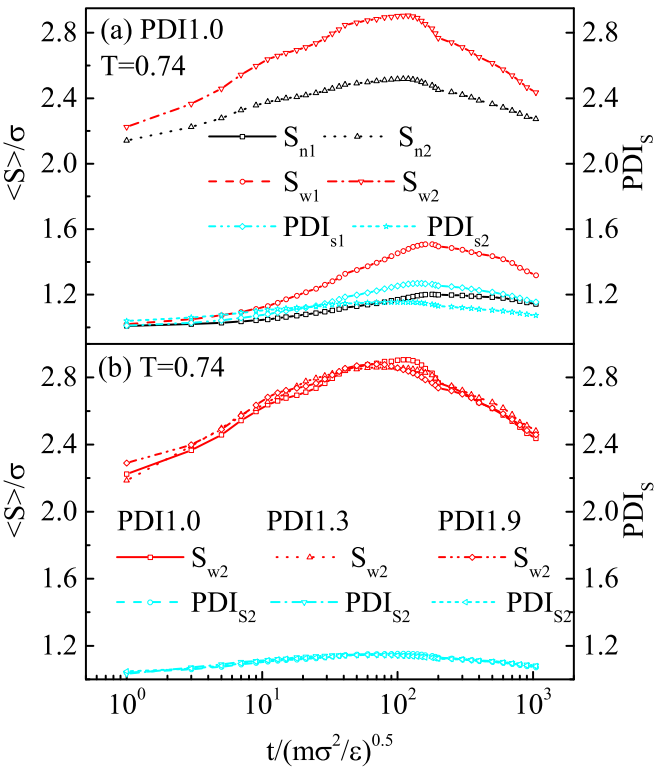

FIG. 6. (a) A comparison between including and not including $s = 1$ in the definition of the average string size and the corresponding polydispersity index of the string size PDI_S. (b) The influence of chain length polydispersity on the string size $\langle S_{w2} \rangle$ and PDI_S. The PDI values for SZ distribution are 1.3 and 1.9.

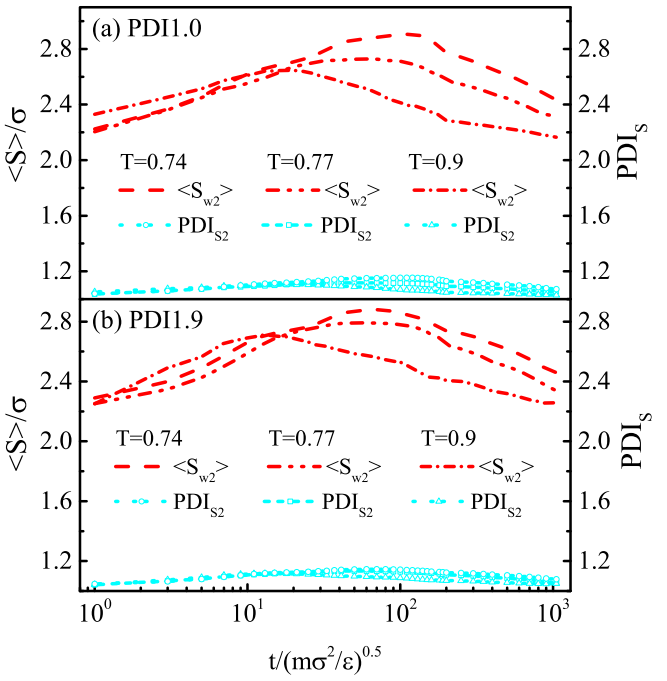

FIG. 7. The temperature dependence of the string size $\langle S_{w2} \rangle$ and the distribution PDI_S for monodisperse (a) and polydisperse (b) systems.

D. Heterogeneous dynamics

The above analyses of string size have given us a physical picture of the dynamic heterogeneity of polymeric glass formers. To further understand the effects of chain length polydispersity on dynamic heterogeneity in our systems, we first partition the monomers of each polymer system into six equal groups with index G0–G5 according to the monomer tags in the simulations both for monodisperse and polydisperse systems in the same way. For polydisperse systems, a larger number (for example, G5) means that the monomers belong to longer chains. It can be seen in Fig. 8 that for the monodisperse system, $g_0(t)$ of monomers in different chains have the same behavior. However, various groups in polydisperse systems move differently: monomers belonging to longer chains move slower. These results clearly illustrate that chain length polydispersity affects the motion distribution of monomers in the systems.

To quantify the difference in dynamic heterogeneity between polymer systems with various PDIs, we have measured the non-Gaussian parameter for monomers [25], which is defined as

$$\alpha_2 = \frac{3\langle g_i^4(t)\rangle}{5\langle g_i^2(t)\rangle^2} - 1. \tag{15}$$

Here, $g_i(t)$ is the MSD of the ith monomer at time t. The non-Gaussian parameter α_2 quantifies the deviation of the monomer motion distribution from the Gaussian distribution of simple diffusive motion. A larger α_2 indicates that the motion distribution of monomers is more heterogeneous [2]. From Fig. 9, we can observe that there is a peak for the non-Gaussian parameter, which is on time scales between α and β relaxation time [25,57]. The position of the peak is at the time when a monomer begins to break out of the cage formed by nearby monomers [2]. As shown in Fig. 9(b), the magnitude of the peak increases and the position of the peak shifts to a larger time scale upon cooling, which implies an enhanced dynamic heterogeneity [25]. At the same temperature, there is a similar but much weaker trend with increasing PDI at the same chain length distribution form, as shown in Fig. 9(a). When focusing on the right side of the peak, compared with monodisperse systems, we find a rather sharp jump in the non-Gaussian parameter, implying a considerable enhanced dynamic heterogeneity at these time scales. α_2 increases quickly with the PDI in the same time range, suggesting that the dynamic heterogeneity of monomer motion after breaking out of the cage is enhanced dramatically by increasing the chain length polydispersity. After breaking out of the cage, the monomers can explore larger regions and can feel more the influence of chain length polydispersity. This alters the monomer dynamic heterogeneity very much, but it has only a weak influence on the average monomer motion. As shown in Fig. 9(b), the α_2 value for polydisperse systems at the right side of the peak decreases instead of increasing upon cooling at the same time range, which is obviously distinct from classical dynamic heterogeneity behavior for monodisperse polymer systems around the peak. The effect of chain length polydispersity on α_2 is related not only to

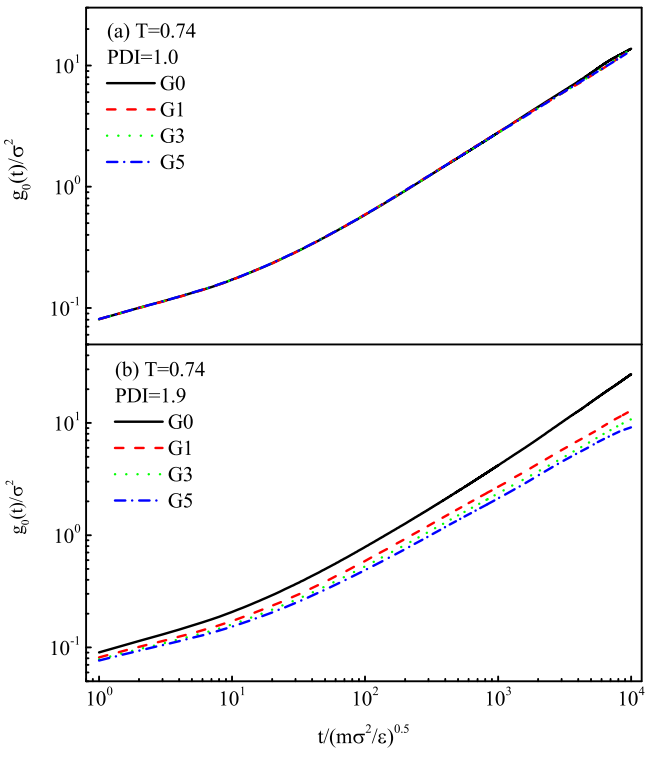

FIG. 8. MSD of different groups in monodisperse (a) and polydisperse (b) systems. The larger number means that the monomers belong to longer chains for polydisperse systems. For clarity, we leave out the data of G2 and G4.

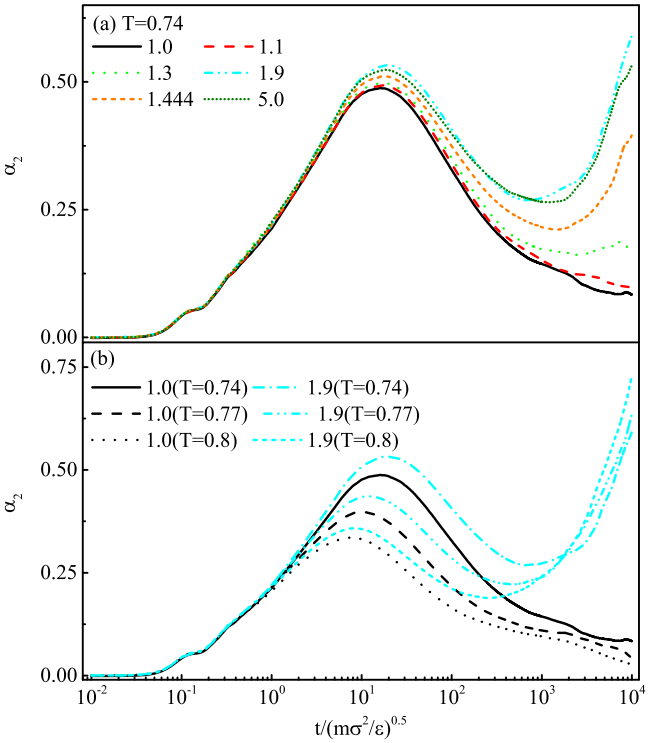

FIG. 9. Non-Gaussian parameters for systems with various polydispersity at the same temperature (a) and at different temperatures (b). The PDI values for SZ distribution are 1.1, 1.3, and 1.9. The PDI values for bimodal distribution are 1.444 and 5.0.

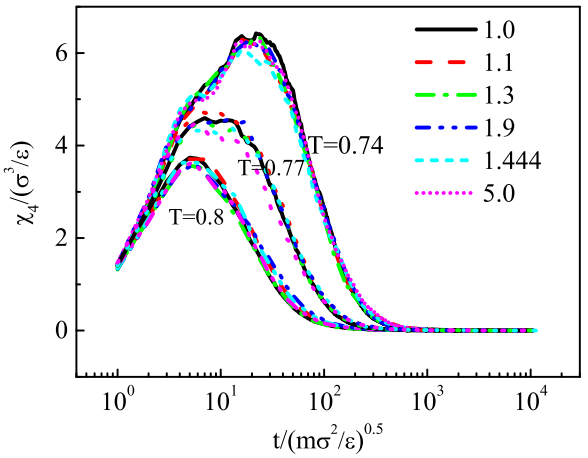

FIG. 10. The variation of four-point susceptibilities with temperature and PDI. The PDI values for SZ distribution are 1.1, 1.3, and 1.9. The PDI values for bimodal distribution are 1.444 and 5.0.

the PDI value but also to the chain length distribution form, just as the effect of chain length polydispersity on $g_3(t)$ (cf. Fig. 4).

The non-Gaussian parameter α_2 reflects the behavior of temporarily localized ("caged") monomers. To determine the influence of chain length on the transient spatial correlation between temporarily localized monomers, we calculate the four-point susceptibility $\chi_4(t)$, which also describes the heterogeneity of the systems:

$$\chi_4(t) = \frac{\beta V}{N^2}[\langle Q^2(t)\rangle - \langle Q(t)\rangle^2],$$

$$Q(t) = \sum_{i=1}^{N} w[|r_i(t) - r_i(0)|]. \quad (16)$$

Here, $r_i(t)$ is the position of the ith monomer at time t, β is $1/(k_B T)$, $w(x)$ is a function that is unity for $x \leqslant a = 0.3$ and zero otherwise, and $Q(t)$ is the number of monomers that remain within a distance a of their original positions at time t, which describes the configuration overlap through a period time t [26,27]. The height of the peak is related to the volume with which the local structural relaxation processes are correlated [16], therefore it corresponds to a dynamic length scale. As shown in Fig. 10, the peak value of $\chi_4(t)$ increases upon cooling, implying a growing correlation length. The peak position shifts to larger time scales upon cooling, suggesting a slower relaxation. Although there are some fluctuations, we can conclude that the transient spatial correlation between temporarily localized monomers $\chi_4(t)$ and the corresponding dynamic correlation length are not affected by chain length polydispersity.

IV. DISCUSSION AND CONCLUSIONS

In this paper, we present the results of molecular-dynamics simulations for polydisperse polymer systems, and we show that the glass transition temperature T_g is not influenced by molecular-weight polydispersity. The segment dynamics and dynamic heterogeneity of supercooled polydisperse polymer systems suggest that T_g only relates to the local relaxation of the polymer chains. The analysis of the stringlike cooperative motion implies the local nature of the glass transition. In the study of the mass dependence of the T_g nanoconfinement effect, Torkelson and co-workers have found that the polydisperse polystyrene sample (made with a blend of high and very low molecular-weight polystyrene, i.e., bimodal distribution) has a very similar T_g to that of a nearly monodisperse polystyrene system. This result suggests that chain end segregation, which is different for systems with different chain length polydispersity, has very little effect on the local relaxation behavior (T_g nanoconfinement effect) [58]. Analogously, the chain length distribution may not be able to affect the glass transition effectively since T_g is primarily dependent on the local relaxation of polymer segments. Therefore, our results emphasize that bulk T_g is determined by chain end concentration (number-average chain length), rather than by chain end segregation (polydispersity). Paul and Smith stated that monomers were caged before realizing that they belong to chains in the classical bead-spring model, which leads to a similar T_c for the classical bead-spring model and Lennard-Jones "atomic" liquids [4]. Likewise, monomers in situations with the same chain end concentration (which is determined by $\langle N\rangle$) may not feel the existence of chain length distribution when the temperature approaches T_g.

Our results imply that polymers with a different mass-average molecular weight can have the same T_g value if they have the same number-average molecular weight. The more relevant factor for the mass dependence of T_g is the number-average one rather than the mass-average one. Recently, Zaccone and Terentjev proposed a model to explain the melting transition mechanism of amorphous solids in terms of the lattice energy lost to this nonaffine motion [59]. In their work, T_g is determined based on the sharp drop of the low-frequency shear modulus upon raising the temperature from the low-temperature glass. The average number of connectivities per atom is defined as z. The connectivity due to van der Waals potentials (nonbonded potential) is defined as z_{LJ}. Another important contribution to z is from covalent bonds, defined as z_{co}. For polymer chains of n units, $z_{\mathrm{co}} = 2(1 - 1/n)$. The total constraints from other monomers is therefore $z = z_{\mathrm{co}} + z_{\mathrm{LJ}}$. According to the theory of Zaccone and Terentjev, when z exceeds the critical value z_c, the system loses its fluidity and becomes rigid and glassy; when z is smaller than z_c, materials are unstable and unable to support shear or tensile stress. The temperature at which $z = z_c$ can be determined as the glass transition temperature T_g. Zaccone and Terentjev found that for polymers, $z_c = (12 - 4)z_{\mathrm{co}}$. As z_{co} is determined by the degree of polymerization n, Zaccone and Terentjev obtained a relation between molecular weight and T_g for polymers, which recovers the Fox-Flory equation (for more details, see Ref. [59]). As this approach shows, it is evident that T_g is controlled by a global rigidity transition that depends on the average connectivity per atom, z_{co}. In our studies, we find that $z_{\mathrm{co}} = 1.833$ for $\langle N\rangle = 12$ and $z_{\mathrm{co}} = 1.95$ for $\langle N\rangle = 40$, and polydispersity has little influence on the value of z_{co}. Therefore, z_{co} is determined by the number average length $\langle N\rangle$: $z_{\mathrm{co}} = 2(1 - 1/\langle N\rangle)$. What matters for z_{co} is the number average bond number per chain, rather than its fluctuations due

to the polydispersity. According to these theoretical results and our analyses, chain length polydispersity should hardly affect T_g.

To conclude, although molecular-weight polydispersity affects the processing properties of polymer materials, our results show that it has very little influence on the glass transition temperature. Deliberate control over molecular-weight distribution may largely improve the polymer processing properties while keeping the mechanical properties unchanged.

ACKNOWLEDGMENTS

This work is subsidized by the National Basic Research Program of China (973 Program, 2012CB821500), and supported by the National Science Foundation of China (21534004). We also acknowledge the support from Jilin Province Science and Technology Development Plan (20140519004JH). Z.Y.L. is also grateful to the Wenner-Gren Center Foundation for Scientific Research for financial support during his time as a visiting scientist in Sweden.

[1] J. L. Barrat, J. Baschnagel, and A. Lyulin, Soft Matter **6**, 3430 (2010).
[2] J. Baschnagel and F. Varnik, J. Phys. Condens. Matter **17**, R851 (2005).
[3] S. Y. Shang and Z. P. Fang, Chin. J. Polym. Sci. **31**, 1334 (2013).
[4] W. Paul and G. D. Smith, Rep. Prog. Phys. **67**, 1117 (2004).
[5] P. G. Debenedetti and F. H. Stillinger, Nature (London) **410**, 259 (2001).
[6] L. Berthier and G. Biroli, Rev. Mod. Phys. **83**, 587 (2011).
[7] G. Biroli and J. P. Garrahan, J. Chem. Phys. **138**, 12A301 (2013).
[8] A. Cavagna, Phys. Rep. **476**, 51 (2009).
[9] N. A. Lynd, M. A. Hillmyer, and M. W. Matsen, Macromolecules **41**, 4531 (2008).
[10] W. Minoshima, J. L. White, and J. E. Spruiell, Polym. Eng. Sci. **20**, 1166 (1980).
[11] S. G. Hatzikiriakos, Prog. Polym. Sci. **37**, 624 (2012).
[12] M. D. Ediger, C. A. Angell, and S. R. Nagel, J. Phys. Chem. **100**, 13200 (1996).
[13] N. A. Rorrer and J. R. Dorgan, Macromolecules **47**, 3185 (2014).
[14] A. L. Agapov and A. P. Sokolov, Macromolecules **42**, 2877 (2009).
[15] V. N. Novikov and E. A. Rössler, Polymer **54**, 6987 (2013).
[16] L. Berthier, Physics **4**, 42 (2011).
[17] S. Karmakar, C. Dasgupta, and S. Sastry, Annu. Rev. Condens. Matter Phys. **5**, 255 (2014).
[18] G. Adam and J. H. Gibbs, J. Chem. Phys. **43**, 139 (1965).
[19] V. Lubchenko and P. G. Wolynes, Annu. Rev. Phys. Chem. **58**, 235 (2007).
[20] C. Donati, J. F. Douglas, W. Kob, S. J. Plimpton, P. H. Poole, and S. C. Glotzer, Phys. Rev. Lett. **80**, 2338 (1998).
[21] M. Aichele, Y. Gebremichael, F. W. Starr, J. Baschnagel, and S. C. Glotzer, J. Chem. Phys. **119**, 5290 (2003).
[22] L. Berthier, G. Biroli, J. P. Bouchaud, L. Cipelletti, D. El Masri, D. L'Hote, F. Ladieu, and M. Pierno, Science **310**, 1797 (2005).
[23] M. D. Ediger, Annu. Rev. Phys. Chem. **51**, 99 (2000).
[24] H. C. Andersen, Proc. Natl. Acad. Sci. (USA) **102**, 6686 (2005).
[25] W. Kob, C. Donati, S. J. Plimpton, P. H. Poole, and S. C. Glotzer, Phys. Rev. Lett. **79**, 2827 (1997).
[26] S. C. Glotzer, V. N. Novikov, and T. B. Schrøder, J. Chem. Phys. **112**, 509 (2000).
[27] N. Lacevic, F. W. Starr, T. B. Schrøder, and S. C. Glotzer, J. Chem. Phys. **119**, 7372 (2003).
[28] G. S. Grest and K. Kremer, Phys. Rev. A **33**, 3628(R) (1986).
[29] B. Schnell, H. Meyer, C. Fond, J. P. Wittmer, and J. Baschnagel, Eur. Phys. J. E **34**, 97 (2011).
[30] S. J. Xie, H. J. Qian, and Z. Y. Lu, J. Chem. Phys. **140**, 44901 (2014).
[31] M. Bernabei, A. J. Moreno, and J. Colmenero, J. Chem. Phys. **131**, 204502 (2009).
[32] M. Bernabei, A. J. Moreno, and J. Colmenero, Phys. Rev. Lett. **101**, 255701 (2008).
[33] J. Rottler and M. O. Robbins, Phys. Rev. Lett. **89**, 195501 (2002).
[34] C. Bennemann, C. Donati, J. Baschnagel, and S. C. Glotzer, Nature (London) **399**, 246 (1999).
[35] H. Lee, R. M. Venable, A. D. MacKerell Jr., and R. W. Pastor, Biophys. J. **95**, 1590 (2008).
[36] P. J. Steinhardt, D. R. Nelson, and M. Ronchetti, Phys. Rev. B **28**, 784 (1983).
[37] Y. L. Zhu, H. Liu, Z. W. Li, H. J. Qian, G. Milano, and Z. Y. Lu, J. Comput. Chem. **34**, 2197 (2013).
[38] J. Buchholz, W. Paul, F. Varnik, and K. Binder, J. Chem. Phys. **117**, 7364 (2002).
[39] Z. Dobkowski, Eur. Polym. J. **18**, 563 (1982).
[40] J. C. Conrad, F. W. Starr, and D. A. Weitz, J. Phys. Chem. B **109**, 21235 (2005).
[41] S. J. Xie, H. J. Qian, and Z. Y. Lu, J. Chem. Phys. **137**, 244903 (2012).
[42] C. A. Angell, K. L. Ngai, G. B. McKenna, P. F. McMillan, and S. W. Martin, J. Appl. Phys. **88**, 3113 (2000).
[43] F. Varnik, J. Baschnagel, and K. Binder, Phys. Rev. E **65**, 021507 (2002).
[44] K. Binder, J. Baschnagel, and W. Paul, Prog. Polym. Sci. **28**, 115 (2003).
[45] S. Peter, H. Meyer, and J. Baschnagel, J. Polym. Sci. Part B: Polym. Phys. **44**, 2951 (2006).
[46] S. Peter, H. Meyer, J. Baschnagel, and R. Seemann, J. Phys. Condens. Matter **19**, 205119 (2007).
[47] W. Götze, *Complex Dynamics of Glass-Forming Liquids: A Mode-Coupling Theory: A Mode-Coupling Theory* (Oxford University Press, Oxford, 2008), Vol. 143.
[48] R. A. Riggleman, K. Yoshimoto, J. F. Douglas, and J. J. de Pablo, Phys. Rev. Lett. **97**, 045502 (2006).
[49] S. J. Xie, H. J. Qian, and Z. Y. Lu, Polymer **56**, 545 (2015).
[50] S. J. Xie, H. J. Qian, and Z. Y. Lu, J. Chem. Phys. **142**, 074902 (2015).

[51] A. V. Lyulin, N. K. Balabaev, and M. A. J. Michels, Macromolecules **35**, 9595 (2002).
[52] R. Mao, J. Tang, B. Swanson, J. Otte, M. Zakora, K. Qvist, W. Kalt, J. McDonald, H. Donner, X. Lou *et al.*, J. Food Sci. **65**, 374 (2000).
[53] S. W. Provencher, Comput. Phys. Commun. **27**, 213 (1982).
[54] S. W. Provencher, Comput. Phys. Commun. **27**, 229 (1982).
[55] F. W. Starr, J. F. Douglas, and S. Sastry, J. Chem. Phys. **138**, 12A541 (2013).
[56] Y. Gebremichael, T. B. Schrøder, F. W. Starr, and S. C. Glotzer, Phys. Rev. E **64**, 051503 (2001).
[57] M. Vogel, Macromolecules **41**, 2949 (2008).
[58] C. J. Ellison, M. K. Mundra, and J. M. Torkelson, Macromolecules **38**, 1767 (2005).
[59] A. Zaccone and E. M. Terentjev, Phys. Rev. Lett. **110**, 178002 (2013).